SMGroup

SM Journal of Biometrics & Biostatistics

Research Article

Characteristics of Photosynthetic Active Radiation (PAR) Through Statistical Analysis at Larnaca, Cyprus

Pashiardis S[1], Kalogirou SA [1]* and Pelengaris A[2]

[1]*Department of Mechanical Engineering and Materials Science and Engineering Cyprus University of Technology, Limassol, Cyprus*

[2]*Department of Cyprus Public Works, Ministry of Transport Communications and Works, Strovolos Avenue 165, 2048 Strovolos, Cyprus*

Article Information

Received date: May 25, 2017
Accepted date: Jun 09, 2017
Published date: Jun 16, 2017

***Corresponding author**

SA Kalogirou, Department of Mechanical Engineering and Materials Science and Engineering Cyprus University of Technology, Limassol, Cyprus;
Tel: +357-2500-2621; Fax: +357-2500-2637; Email: soteris.kalogirou@cut.ac.cy

Keywords Photosynthetic active radiation; Statistical analysis; Temporal and spatial variation; Modelling PAR; Cyprus

Abstract

Measurements of Photosynthetically Active Radiation (PAR) and global solar radiation at Larnaca (a coastal site in Cyprus) during the period 3013-2015 were used to investigate the seasonal characteristics of PAR and PAR/G ratio (PAR fraction or fFEC). PAR showed seasonal features with higher values in summer and lower values in winter. The annual mean values of PPFD and fFEC being 40.3 mol m^{-2} d^{-1} and 2.03 mol M J^{-1}, respectively. Monthly average daily PAR increased from 19.1 mol m^{-2} d^{-1} (in December) to 59.6 mol m^{-2} d^{-1} (in June).The monthly daily average of fFEC remained almost constant throughout the year at Larnaca. The spatial variability of PAR was also investigated using measurements from other four sites with different climate characteristics. The annual mean daily PAR value ranged between 31.7 to 40.0mol m^{-2} d^{-1}. The highest values are recorded in the coastal stations (Larnaca and Paralimni). The annual average value of fFEC at the five observation sites ranged from 1.82 mol MJ^{-1} to 2.03 mol MJ^{-1}, in accordance to what is observed in most parts of the world. The highest appeared in the coastal sites of Larnaca and Paralimni due to the presence of high water vapour atmospheric concentrations. Elevation plays a significant role on the values of the above variables. As a general trend, fFEC followed the order Clear<Partly cloudy<Cloudy. In all cases fFEC was decreased with elevation but with a different rate. Three linear or multilinear and three power law models were tested and validated under all sky conditions. All the models showed high coefficients of determination (R^2) (close to 1), which indicates that the proposed models are suitable for predicting hourly PAR values. The linear and multilinear models (models 1 to 3) have the same coefficient of determination (0.996). The relative error values for the first five models ranged between 3.3% and 4.5%, while the sixth model showed higher relative error (8.4%).

Introduction

Photosynthetically Active Radiation (PAR) is defined as the electromagnetic radiation in the waveband between 400 and 700 nm, which can be used as the source of energy for photosynthesis by green plants [1-3]. PAR is a key variable in a wide range of ecophysiological models, both at leaf photosynthesis level [4] and crop production level [5]. Precise estimation of incident PAR is therefore essential in assessing and modelling plant growth and biological production management in different vegetative ecosystems. Monteith suggested that the net primary production under non-stressed conditions is linearly related to the amount of PAR that is absorbed by the green foliage [6,7].

The radiation incident on a plant canopy arrives as direct and diffuse fluxes. The direct flux is formed by photons having passed through the atmosphere unscattered, whereas the diffuse flux consists of photons scattered by air molecules, aerosols particles or clouds. Depending on aerosol load and solar elevation, the ratio of diffuse PAR to global PAR irradiance on a horizontal surface ranges between 20% and 40% [8]. Only photons absorbed by the canopy can be used for photosynthesis. A constant coefficient of absorbed to incident flux density of 0.85 has been proposed for radiation use efficiency calculations [6,9].

Even though PAR is extremely important, it is often not measured in most meteorological stations. Therefore, it has to be estimated from the commonly measured global solar radiation (*G*). It is expressed either in terms of Photosynthetic Photon Flux Density (PPFD, μmol m^{-2} s^{-1}), since photosynthesis is a quantum process, or in terms of Photosynthetic Radiation Flux Density (PAR irradiance, W m^{-2}), which is more suitable for energy balance studies. It can be also expressed as (a) a fractional energy of PAR to global solar radiation (*f*PAR) [10,11], (b) as a fraction of photon flux to energy conversion (*fFEC*, μmol J^{-1} or mol MJ^{-1}) [12-14], or (c) as a lost PAR energy (*LPR*) in the atmosphere, i.e., the percentage of extraterrestrial PAR energy lost in the atmosphere when solar radiation penetrates from the extraterrestrial system to the ground [15].

The classical Conversion Factor (*cf*) of 4.57 μmol J^{-1} (or μmol s^{-1} W^{-1}) proposed by McCree [1,16] is used to convert PAR photon flux into its energy alternative (i.e., PAR*E*). This is also confirmed by later studies [17]. For the diffuse component, under blue sky an average value of 4.28 μmol J^{-1}

was reported [8]. In the presence of clouds the factor increases with increasing cloud cover from 4.24 μmol J^{-1} to the constant value for global radiation of 4.57 μmol J^{-1} under overcast sky [17].

The ratio of PAR to shortwave irradiance at the top of the atmosphere equals 38.8% and is based on the solar constant of 1367 W m^{-2} [18]. Using the value of $PPFD_0$ as 2443.3 μmol m^{-2} s^{-1} (i.e., the photosynthetic photon flux density solar constant at the top of the atmosphere on a surface perpendicular to sunrays), we obtain that the ratio of PAR to shortwave irradiance outside the atmosphere equals 4.57 μmol J^{-1}, exactly that proposed by McCree [1]. Spitters et al. [19] have proposed a higher solar constant for PAR which is equal to 2776.4 μmol m^{-2} s^{-1}.

PAR is mainly estimated as a constant fraction of broadband solar irradiance. The fraction of PAR in global shortwave irradiation (*f*PAR) varies little and is usually between 40% and 50% [20,21]; values above 50% occur under very low sun, thick cloud cover or rain [22]. Some variation in *f*PAR with elevation above sea level is expected, but this variation is difficult to detect [8]. However, Wang et al. [23] noted an increasing trend with altitude, of about 3.6% per km for hourly values under clear skies, using measurements at 550, 900 and 1500 m above sea level. An inverse trend was found for hourly *f*PAR under cloudy weather conditions: *f*PAR decreased at a rate of 1.8% per km.

Several methods exist for modeling PAR and its components: (a) the radiative transfer method which takes into account several atmospheric processes such as Rayleigh scattering, water vapour, ozone absorption and aerosol load [8,18,24-29]; (b) a method of using artificial neural network [30]; (c) a method of estimation of PAR through satellite observations [31-35]; (d) statistical models which can be subdivided into four different groups depending on their complexity and the selected variables: (i) Semi-parametric partitioning diffuse models which are based on the relationship of the diffuse PAR fraction k_{dp} (ratio of the diffuse-to-global PAR solar radiation) with the fractional transmission of global PARk_{PAR} (ratio of global PAR-to-extraterrestrial solar PAR) [11,21,36]; (ii) Empirical models which are based on selected sky condition parameters which affect PAR such as the clearness of the sky (ε), the brightness of the skylight (Δ), the global solar radiation, the solar zenith angle, the optical air mass and the dew point temperature or vapour pressure. The sky clearness parameter, ε, depends on the cloud and aerosol amount. The skylight brightness parameter, Δ, depends on the aerosol burden and the cloud thickness [2,12,37,38]; (iii) PAR parameterization models based on the evaluation of the attenuation factors which affect the transmissivity of PAR through the atmosphere [39,40]; (iv) Simple linear or multilinear models based on parameters routinely measured in meteorological stations. The variables are chosen from their presumed influence on PAR radiation, such as global solar radiation, clearness index (k_t), Solar Zenith Angle (SZA), sunshine duration and vapour pressure [14,15,30].

Details about the levels of the shortwave radiation components at Athalassa (Cyprus) are given by Jacovides et al. [41]. Petrakis et al. [42] presented the 'Typical Meteorological Year' for Nicosia (Cyprus). An assessment of the solar radiation climate of the Cyprus environment was recently presented by Kalogirou et al. [43] using statistical analysis and inter-comparison of the solar global radiation at two sites in Cyprus, one at Athalassa-inland location and second one at Larnaca-coastal location, based on measurements of 21 months at both sites. Recently, Pashiardis et al. [44] have analysed the short wave irradiation using 3 years of data based on the concept of clearness index. Furthermore, Jacovides et al. have studied various aspects of PAR radiation at Athalassa, Cyprus, including the implementation of different types of models [3,21,30,45]. Tymvios et al. [46] have also analysed the diurnal variation of direct and diffuse PAR radiation components at Athalassa, using relevant measurements during the period 2000-2002.

The present analysis aims to (a) quality control of the data; (b) investigate seasonal and diurnal patterns of PAR-related values (PPFD, PARE, *fPAR, fFEC*, LPR) throughout the year; (c) obtain statistical relationships between PAR and different radiation components; (d) estimate the frequency distributions of PAR irradiances; (e) compare the levels of PAR-related values with a number of stations operated in Cyprus and assess their variability with elevation; and (f) develop and testing empirical models to precisely estimate hourly and daily PAR values.

Measurements and Methodology

Continuous measurements of *G*, PAR, air temperature (*T*) and Relative Humidity (RH) were taken from the meteorological station of Larnaca Airport which is near the coast. Data were collected from January 2013 to December 2015 (i.e., 3years). The sensors readings were taken every 10 s, with the average and extreme values calculated every 10 min. A Campbell Scientific Instruments data-logger (Model CR10) monitors and stores the data at 10-min and hourly intervals. The stored data are downloaded to a desktop computer periodically. The data refer to the Local standard Time (*LST=GMT+2*).

Measurements of broadband solar irradiance were made with Kipp & Zonen pyranometer (CM11), while the Photosynthetic Flux Density (PPFD) was measured with the quantum sensor PQS1 of Kipp & Zonen which outputs data in photobiological units of micromoles per square meter per second. All sensors are factory calibrated, in accordance with the World Radiometric Reference (WRR). Global radiation instruments are calibrated outdoors against standard references at irregular time intervals during the study period. The errors involved in the radiation measurements are found to be no less than ± 2% for the normal incidence beam irradiance and ± 3% for the global irradiance. The PAR sensor has an error of ± 3% under natural light. Due to cosine response issues of the instrumentation, this analysis is limited to cases with solar elevation angles $\alpha_s > 7^0$. The hourly and daily data were further checked for inconsistencies to eliminate problems associated with questionable measurements.

About 2% of the data values are missing because of some problems with the instruments and some defects and maintenance in the data acquisition systems. The validity of the individual measurements was checked in accordance with *WMO* recommendations (1987) [47] and other tests proposed by various authors [48-50]. Details about the quality control procedures for solar radiation measurements are given by Pashiardis and Kalogirou [51]. The theoretical basis of PAR data quality control is based on the following criteria [52]:

- Firstly, measured PAR values must be lower than the PAR flux at the top of the atmosphere, i.e. the extraterrestrial PAR flux (PARE<PARE_0);
- Secondly, daily PAR/*G* values ($fFEC_d$) must fall between 1.3 and 2.8 mol MJ^{-1}.

Table 1: Geographical coordinates of the stations equipped with *PQS1* Quantum sensor and pyranometer for global solar radiation measurements.

Station	Long. (E)	Lat. (N)	Elevation (m)	Location	Annual Avg. Air Temp. (°C)	Annual Precipitation (mm)
Larnaca	33° 38'	34° 53'	1	Coastal	19.6	332.7
Paralimni	33° 58'	35° 04'	70	Coastal	19.8	352.9
Choulou	32° 33'	34° 52'	316	Inland	17.4	674.0
Kalopanayiotis	32° 49'	35° 00'	584	Inland	17.2	602.5
Farmakas	33° 08'	34° 55'	832	Inland	15.4	635.9

All data that do not meet the conditions specified by the suggested tests are not used in the study. The data passed the above criteria. Finally, there were 22 missing days and therefore a total of 1073 days of data were used in analysis obtained from Larnaca station.

The values of global and photosynthetic active radiation were also compared with the relevant data of other four stations with hourly observations mainly during the period 2013-2016. Table 1 shows details about the geographical coordinates of the measuring stations. All stations are equipped with the same type of Quantum sensor PQS1 of Kipp & Zonen which outputs data in photobiological units. The data from Larnaca during the first two years will be used for the development of the models, while the data of the year 2015 will be used for validation purposes.

Methodology

The magnitudes of Photosynthetic Photon Flux Densities (PPFD) were processed at both the hourly and daily time scales. The hours and days of the studied period have been classified according to the sky conditions. Hourly, k_t and daily, K_T clearness indices were calculated for each hour and day, respectively, during the measurement period, using the following expressions [53]:

$$k_t = G / G_0 \quad (1)$$

$$K_T = G_d / G_{0d} \quad (2)$$

Where G is the hourly global solar irradiation; G_d is the daily global solar irradiation; G_0 and G_{0d} are the hourly and the daily extraterrestrial solar global irradiation on a horizontal surface, respectively, which are given by the following expressions [53]:

$$G_0 = G_{SC} * L * [\sin\phi * \sin\delta + \cos\phi * \cos\delta * \cos\omega_i] \quad (3)$$

$$G_{0d} = (24/\pi) * G_{SC} * L * [\sin\phi * \sin\delta (\pi * \omega_s / 180) + \cos\phi * \cos\delta * \sin\omega_s] \quad (4)$$

Where L is the eccentricity ($L = 1 + 0.033 * \cos(360 * jd / 365)$), jd is the Julian day mumber, ϕ is the latitude of the site, δ is the solar declination angle ($\delta = 23.45 * \sin(360 * (284 + jd) / 365)$), ω_s is the sunset hour angle ($\omega_s = \cos^{-1}(-\tan\phi * \tan\delta)$), G_{sc} is the solar constant (G_{sc}=1367 W m^{-2}), ω_i are the hour angles at the centre of the hour interval. Equation (3) yields extraterrestrial irradiance for one hour centred on the given hour ω_i.

By analogy, the hourly, k_{PAR} and daily K_{PAR}, PAR clearness indices (or PAR transmissivities through the atmosphere) were calculated for each hour and day, respectively, during the measurement period, using the following expressions:

$$k_{PAR} = PAR / PAR_0 \quad (5)$$

$$K_{PAR} = PAR_d / PAR_{0d} \quad (6)$$

The hourly and daily values of extraterrestrial PAR radiation can be estimated with the Eqs (3) and (4). The solar constant of photosynthetic active irradiance (PAR_{sc}) is obtained from Gueymard [54] and is equal to 534.64 W m^{-2} which is equivalent to 2443.3 μmol m^{-2} s^{-1}, using the McCree's conversion factor of 4.57 μmolJ^{-1} to convert hourly PAR photon flux into its energy alternative.

Combined with global solar radiation and simulated extraterrestrial solar radiation, seven PAR related values were developed, i.e., flux density-based PAR (*PPFD*), energy-based PAR (PAR*E*), from-flux-to-energy conversion efficiency (PAR/*G*, *fFEC*), the fraction of PAR energy in the global solar radiation (*f*PAR), the lost PAR*E* percentages (*LPR*) starting from the top of the atmosphere up to the ground level, and the two clearness indices as defined above (k_t and k_{PAR}). These clearness indices are used to assess the attenuation of global solar and PAR radiation in the atmosphere.

The hourly values of *PPFD* are given in μmol m^{-2} s^{-1}, while daily *PPFD* values are the sum of the hourly values expressed in moles m^{-2} d^{-1}. The *fFEC* values are computed as fractions of *PPFD* to global solar radiation over the selected time scale. For the daily *fFEC*, the unit is given in moles per MJ, but for the hourly values it is expressed as μmol J^{-1}. The fraction of PAR to global solar radiation (*f*PAR) at the top of the atmosphere is around 40% [55]. However, more recent measurements estimate this parameter at 39.1% [54]. The percentage of extraterrestrial PAR energy lost in the atmosphere (*LPR*) can be calculated from the following expression:

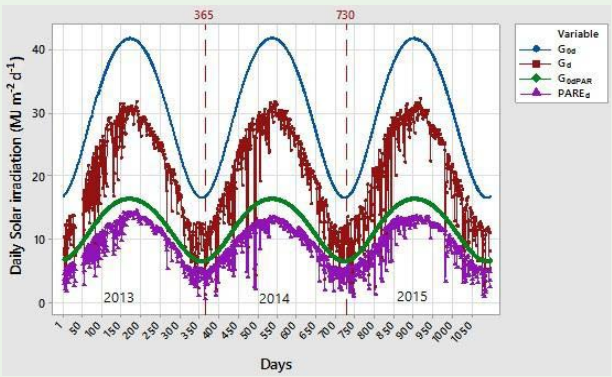

Figure 1: Time series plots of the daily global solar (G_d) and photosynthetic active radiation ($PARE_d$) and their respective extraterrestrial daily radiation values.

Citation: Pashiardis S, Kalogirou SA and Pelengaris A. Characteristics of Photosynthetic Active Radiation (PAR) Through Statistical Analysis at Larnaca, Cyprus. SM J Biometrics Biostat. 2017; 2(2): 1009.

$$LPR = (PARE_0 - PARE) * 100 / PARE_0 \quad (7)$$

In this study the diurnal and seasonal patterns of the above PAR related parameters will be investigated. Furthermore, various models with different complexity will be developed and tested.

The time series plots of the daily global solar and photosynthetic active radiation are shown in Figure 1. The daily values of the respective extraterrestrial radiation for both variables are also shown for comparison. The figure indicates that the daily values of both variables follow the same pattern with the higher values during the summer season and the lower ones during the winter season. The annual mean daily global solar irradiation and PAR*E* are 19.9 MJ m^{-2} and 8.8 MJ m^{-2}, respectively. The maximum daily values reach 32.2 MJ m^{-2} and 14.4 MJ m^{-2}, respectively, both occurring in July.

Results and Discussion

Monthly mean hourly values

The average monthly values and standard errors of global solar irradiance (*G*), global solar extraterrestrial irradiance (G_0), clearness index (k_t), photosynthetic photon flux density (*PPFD*), photosynthetic active irradiance (PAR*E*), extraterrestrial photosynthetic active irradiance (PARE_0), PAR clearness index (k_{PAR}), fraction of PAR irradiance to global irradiance (*f*PAR), flux to energy conversion efficiency (*fFEC*) and lost PAR*E* percentages (*LPR*) are shown in Table 2. The smaller values are occurred during the winter season, due to the presence of clouds. The monthly means of PAR*E* irradiance range from 125 to 258 W m^{-2}, while the mean hourly values of *PPFD* range from 573 to 1186 μmol m^{-2} s^{-1}.

The fraction of PAR to global irradiance (*f*PAR) is relatively constant ranging from 0.432 to 0.455, with the higher values occurring during the winter season. The monthly average of clearness index is higher than 0.65 during the summer months indicating that the atmosphere is mostly clear during this season. During the entire period of measurements the overall mean hourly value of *fFEC* was found to be 2.029 μmol J^{-1}, with the lower values during spring and summer. The percentages of lost PAR*E* (*LPR*) are lower during the summer and autumn season.

Diurnal patterns of monthly mean hourly PAR-related values

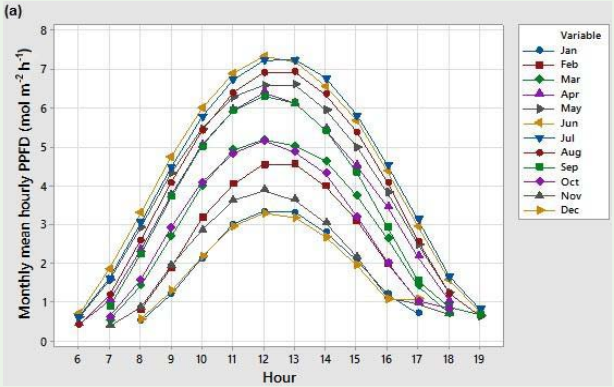

Figure 2a: Monthly mean hourly values for photosynthetic photon flux density (PPFD, mol m^{-2} h^{-1}).

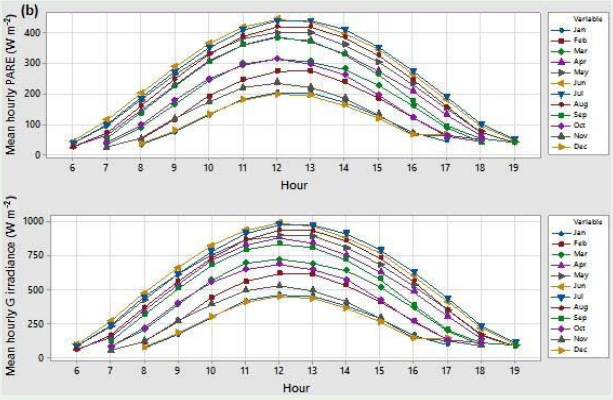

Figure 2b: Monthly mean hourly values for photosynthetic flux density (*PARE*, W m^{-2}) and global solar irradiance (*G*, W m^{-2}).

The monthly averages of hourly PAR values exhibited strong diurnal patterns (Figure 2). Values of *PPFD*, PAR*E*, *f*PAR, *fFEC*, k_{PAR} and *G* were typically low in the early morning, approaching their peaks around the noon hour, and then decreased toward the late afternoon hours. Although *f*PAR and *fFEC* had very conservative daily values when considered on a monthly basis, both exhibited some variability over the course of a day. The average hourly *PPFD* values (Figure 2a) recorded at solar noon varied from 3.27 in December to7.33 mol m^{-2} h^{-1} in June. The respective values of PAR*E* ranged from 191 to 442 W m^{-2} or from 0.69 to 1.59 MJ m^{-2} h^{-1} (Figure 2b). The average hourly global irradiance at solar noon ranged from 450 W m^{-2} in December to 991 W m^{-2} in June (1.62 MJ m^{-2} h^{-1} to 3.57MJ m^{-2} h^{-1}) (Figure 2b). Both *PPFD* and PAR*E* exhibited diurnal trends that were similar to that of global solar radiation, suggesting that both variables are closely associated. Therefore, all PAR-related parameters are influenced by the solar elevation angles and are affected by meteorological parameters such as the turbidity of the atmosphere and clouds.

The means of *fFEC* (Figure 2c) at solar noon ranged from 2.04 μmol J^{-1} in December to 2.06 μmol J^{-1} in June, with an overall mean hourly value of 2.03 μmol J^{-1}. The indicator-lost PAR*E* percentages (*LPR*) follow a different trend. It takes its lower values at the solar noon time and is much lower in the summer than in the winter months. The *LPR* values (Figure 2c) oscillated at solar noon between 32% in December to 14% in June.

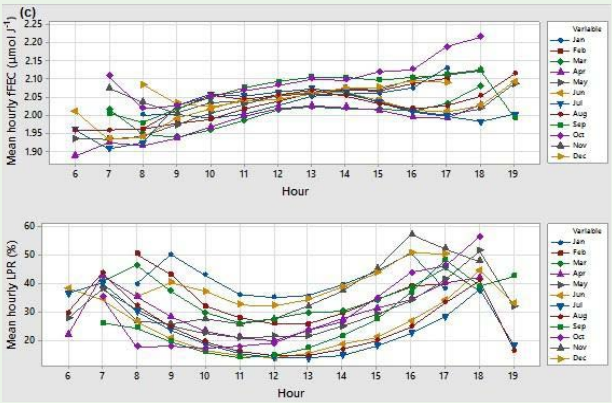

Figure 2c: Monthly mean hourly values for flux-to-energy conversion efficiency (*fFEC*, μmol J^{-1}) and lost *PARE* percentages (*LPR*).

Table 2: Monthly average values and standard errors of global solar irradiance (*G*), global solar extraterrestrial irradiance (G_0), clearness index (k_t), Photosynthetic Photon Flux Density (PPFD), Photosynthetic Active Irradiance (PARE), extraterrestrial photosynthetic active irradiance ($PARE_0$), *PAR* clearness index (k_{PAR}), fraction of *PAR* irradiance to global irradiance (*fPAR*), flux to energy conversion efficiency (*fFEC*) and lost *PARE* percentages (*LPR*) obtained from the hourly data set.

Month	G_M	G_SE	G_0-M	G_0-SE	k_t-M	k_t-SE	PPFD_M	PPFD_SE
	(W m^{-2})	(W m^{-2})	(W m^{-2})	(W m^{-2})			(μmol m^{-2} s^{-1})	(μmol m^{-2} s^{-1})
1	285.8	5.97	474.6	8.24	0.508	0.00677	573.7	11.8
2	397.0	8.48	537.2	9.91	0.576	0.00759	803.4	17.1
3	435.8	8.23	654.2	10.50	0.570	0.00623	861.2	16.2
4	528.8	9.01	713.7	11.40	0.621	0.00551	1047.9	18.1
5	548.8	8.94	757.6	11.40	0.617	0.00504	1099.3	18.2
6	585.9	9.03	721.4	11.80	0.658	0.00413	1185.0	18.6
7	580.6	8.71	731.7	11.60	0.668	0.00351	1178.5	18.2
8	556.5	8.70	741.3	11.10	0.644	0.00415	1132.5	18.0
9	514.7	8.34	660.0	11.00	0.634	0.00464	1067.6	17.6
10	422.3	7.40	580.8	9.60	0.605	0.00551	872.8	15.2
11	335.9	6.22	476.8	8.75	0.553	0.00608	682.5	12.5
12	291.3	5.80	468.6	7.45	0.535	0.00727	588.0	11.5
Year	473.3	2.59	641.1	3.23	0.606	0.00161	957.1	5.3

Month	PARE_M	PARE_SE	$PARE_0$_M	$PARE_0$_SE	kpar_M	kpar_SE	fPAR_M	fPAR_SE	fFEC_M	fFEC_SE
	(W m^{-2})	(W m^{-2})	(W m^{-2})	(W m^{-2})					(μmol J^{-1})	(μmol J^{-1})
1	124.6	2.57	227.9	3.76	0.473	0.0061	0.443	0.0009	2.035	0.0040
2	174.7	3.72	254.1	4.64	0.541	0.0070	0.444	0.0009	2.036	0.0037
3	187.2	3.53	313.9	4.84	0.523	0.0056	0.436	0.0008	1.998	0.0037
4	227.8	3.93	336.7	5.34	0.569	0.0051	0.432	0.0007	1.981	0.0030
5	239.6	3.96	349.7	5.33	0.573	0.0047	0.437	0.0006	2.006	0.0027
6	257.7	4.05	359.7	5.34	0.617	0.0040	0.440	0.0006	2.021	0.0026
7	256.2	3.95	354.9	5.28	0.625	0.0036	0.437	0.0006	2.010	0.0028
8	246.2	3.91	347.5	5.19	0.607	0.0041	0.440	0.0006	2.023	0.0026
9	232.1	3.83	319.0	5.08	0.610	0.0046	0.450	0.0007	2.069	0.0032
10	189.7	3.31	276.7	4.57	0.582	0.0052	0.455	0.0009	2.088	0.0037
11	148.4	2.72	233.8	3.99	0.523	0.0056	0.448	0.0008	2.054	0.0036
12	127.8	2.50	204.8	3.64	0.502	0.0066	0.448	0.0011	2.054	0.0046
Year	208.2	1.15	304.9	1.50	0.590	0.0015	0.442	0.0002	2.030	0.0010

Month	LPR_M	LPR_SE
	(%)	(%)
1	41.40	0.718
2	34.75	0.818
3	35.26	0.631
4	30.47	0.539
5	30.06	0.508
6	25.65	0.383
7	23.83	0.302
8	25.44	0.323
9	24.98	0.516
10	26.73	0.628
11	34.69	0.715
12	38.56	0.777
Year	30.23	0.166

The average hourly values of the PAR clearness index (k_{PAR}) (Figure 2d) at solar noon ranged between 0.554 in January to 0.736 in June, with an overall mean hourly value of 0.567. Finally, the fraction of PAR to global energy (*f*PAR) (Figure 2d) varied from 0.438 in March to 0.448 in July, with an overall mean hourly value of 0.442.

Results of seasonal, annual and sky conditions groupings for different PAR related parameters are shown in Table 3. The characterization of sky conditions was obtained from the classification of the clearness index value, i.e., for $k_t > 0.65$: clear, $0.35 < k_t < 0.65$: partly cloudy and $k_t < 0.35$: overcast sky. *PPFD*, PAR*E* and *G* irradiances show their lower values during overcast sky conditions. On the other hand, *fFEC* and *f*PAR have their higher values under overcast conditions. The hourly ratio of *fFEC* varies from 2.021 (clear days) to 2.179 μmol J^{-1}(overcast days), indicating that this ratio on clear days is 7.9% lower than that on overcast days. Water vapour absorptions take place at longer wavelengths of the spectrum which affect more the broadband global irradiance rather than the PAR component, increasing therefore the *fFEC* values [3,10,12]. Almost similar results were obtained by Jacovides et al. [13] using data from

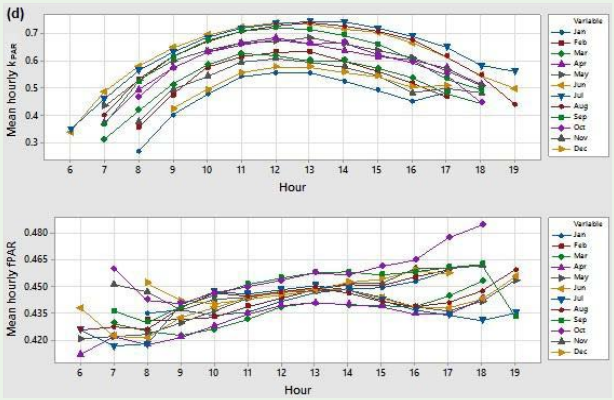

Figure 2d: Monthly mean hourly values for *PAR* clearness index (k_{PAR}) and the fraction of *PAR* energy to global solar radiation.

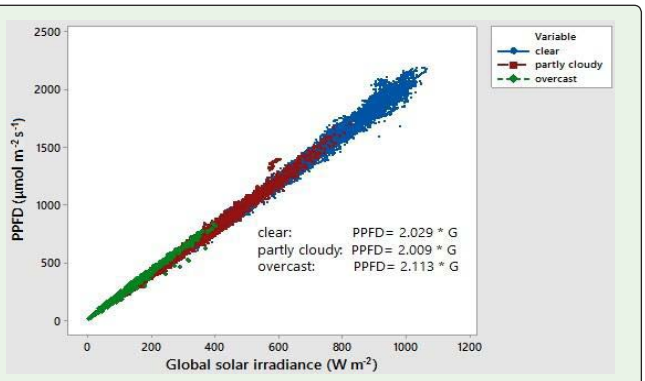

Figure 3: Hourly correlations between spectral (*PPFD*) and broadband irradiance components under clear, partly cloudy and overcast skies at Larnaca.

Athens, Greece. The ratio *f*PAR shows similar variation. It varies from 0.439 on clear days to 0.478 on overcast days, i.e., the ratio on clear days is 8.9% lower than that on overcast days. The indicator *LPR* shows similar trend with the higher values during overcast conditions.

Regarding the seasonal variation, *PPFD*, PAR*E* and *G* irradiances show their higher values in summer. The annual hourly average value of *PPFD* is 3.428 mol m^{-2} h^{-1}, while the respective value in summer is 4.197mol m^{-2} h^{-1}. *fFEC* and *f*PAR show their lower values in spring (1.996 μmol J^{-1} and 0.435, respectively).

The dependence of the hourly *PPFD* values with global solar irradiance for the three sky conditions is also shown in Figure 3. The simple regression line $Y=a*X$ is applied without intercept. The slopes of the fitted lines are shown in the graph. They range from 2.003μmol J^{-1} (clear days) to 2.113 μmol J^{-1} (overcast days). The slope on clear days is 4.2% lower than that in overcast days. Jacovides et al. [3], found for the inland location of Athalassa, slightly lower values than those obtained at Larnaca (coastal location). Similar relationships were established between the hourly PAR irradiance and global solar irradiance. The slopes of the linear fits have the following values: for clear day's *f*PAR=0.441, for partly cloudy day's *f*PAR=0.437 and for overcast day's *f*PAR=0.459. The coefficients of determination are close to 1. The influence of cloudiness through the clearness index on the ratios *fFEC* and *f*PAR is shown in figure 4. The equations associated with this relationship ($Y = aX^b$) are shown in the graph. Similar graphs were obtained by other authors [12, 13].

Accumulated hourly PAR radiation

In the studies of the biological effects of PAR radiation, we require the accumulated PAR solar irradiation through a period of time. The accumulated hourly values of PAR*E* and global solar radiation for an

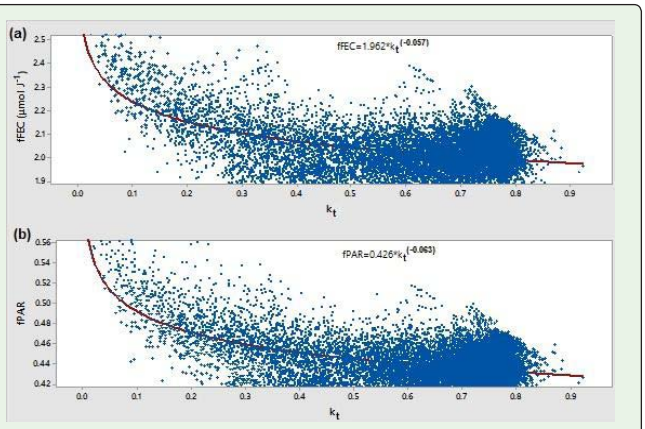

Figure 4: The relationship between the hourly ratios of (a) *fFEC* and (b) *fPAR* vs. clearness index k_t at Larnaca.

Table 3: Photosynthetic active and solar irradiances, and different ratios for seasonal, annual and different sky conditions groupings.

	PPFD	Global	PARE	*f*FEC	*f*PAR	*Kpar*	LPR
Sky conditions	**(mol m^{-2} h^{-1})**	**(W m^{-2})**	**(W m^{-2})**	**(μmol J^{-1})**			**(%)**
Clear	4.934	676.8	297.9	2.021	0.439	0.692	19.5
Partly cloudy	2.200	304.8	132.8	2.003	0.437	0.500	37.7
Overcast	0.979	127.4	59.1	2.179	0.478	0.222	72.4
Seasons							
Winter	2.351	323.3	141.8	2.043	0.445	0.521	38.4
Spring	3.614	504.4	218.2	1.996	0.435	0.575	31.9
Summer	4.197	574.3	253.4	2.018	0.439	0.601	25.0
Autumn	3.088	416.2	186.5	2.072	0.452	0.586	29.5
Annual	3.428	470.3	206.9	2.030	0.442	0.587	30.4

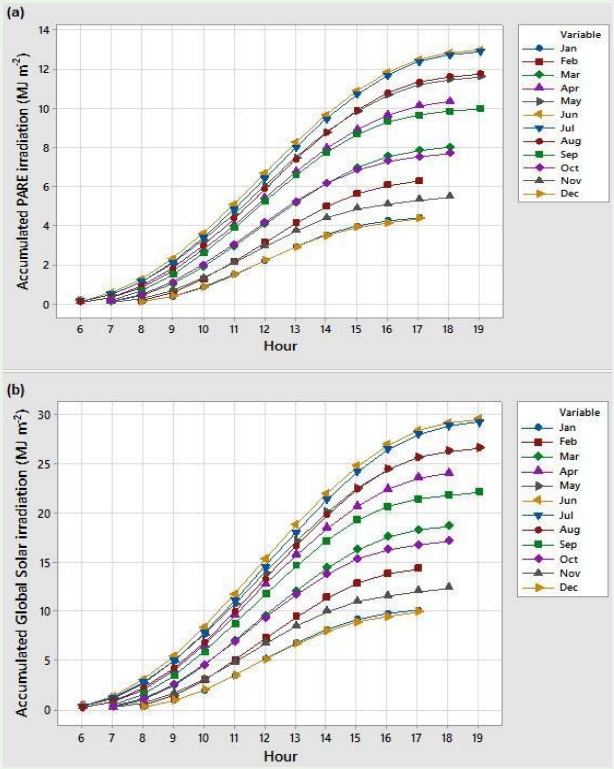

Figure 5: Accumulated (a) *PAR* and (b) *G* irradiation (MJ m^{-2}) for an average day of each month of the year at Larnaca.

average day of each month are shown in figure 5a and 5b, respectively. It can be seen that the highest value for PAR irradiation was produced in July, with a daily average of about 13 MJ m^{-2}. On the other hand, in January and December the average irradiation received was a minimal of about 4.4 MJ m^{-2}. The accumulated PAR irradiation received in an average year is 3222 MJm^{-2}. The respective accumulated global solar irradiation received in an average year is 7324 MJ m^{-2} (Figure 5b).

Frequency distribution of PAR irradiances

The cumulative density functions (*CDF*) of the hourly PAR and *G* irradiances as well as the *PPFD* for the whole period of measurements

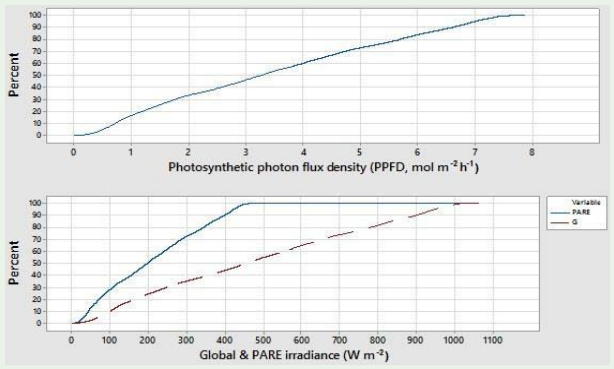

Figure 6: Cumulative density functions (*CDF*) of the photosynthetic photon flux density (*PPFD*, mol m^{-2} h^{-1}), hourly *PARE* and *G* solar irradiances(W m^{-2}) at Larnaca.

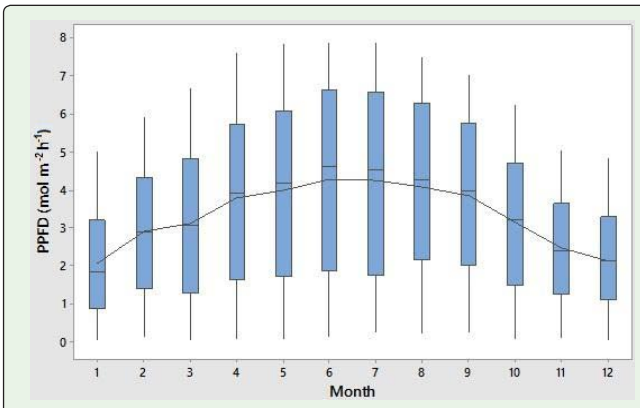

Figure 7: Box plots of the hourly *PPFD* values (mol m^{-2} h^{-1}) for each of the month at Larnaca. The curve shows the monthly mean values.

are shown in figure 6. Figure 6a indicates that in 60% of the hourly values the *PPFD* are lower than 4 mol m^{-2} h^{-1}. Regarding Figure 6b, for the same probability level, the hourly PAR*E* irradiances are lower than 245 W m^{-2} while the hourly *G* irradiances are lower than 560 W m^{-2}.

The variation of the hourly *PPFD* values on a monthly basis is shown with the graph of boxplots (Figure 7). The box plot gives information about the mean of each month as well as the 1st (25%), 2nd (medians) (50%), 3rd (75%) quartiles and the extreme values of the given variable. The means and the medians are very close.

Distribution of monthly mean daily PAR-related parameters

The time series plots of the daily global solar and photosynthetic active radiation including their respective extraterrestrial daily radiations are shown in figure 1. The time series plots of the daily ratios of *f*PAR and the relevant clearness indices of solar (K_T) and PAR radiation (K_{PAR}) are shown in Figure 8a. The *f*PAR ratio is relatively constant with occasional variations throughout the year. In contrast, the clearness indices show high variability at the beginning and end of the year. Daily trends of *fFEC* are shown in Figure 8b. The variability of this ratio is again small. Its mean annual value is 2.029 mol MJ^{-1}. Some outliers are observed in the years 2014 and 2015.

Daily averages for each Julian day and monthly averages have been calculated. Figure 9 shows the results of these calculations. The greatest fluctuations occur in spring and winter seasons. It can be

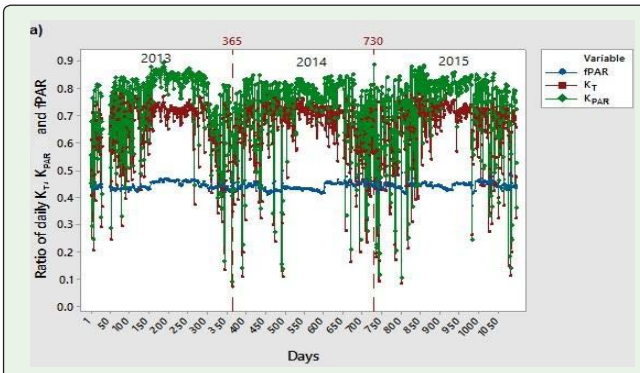

Figure 8a: Time series plots of the daily ratios of *fPAR* and the relevant clearness indices of solar (K_T) and *PAR* radiation (K_{PAR}) at Larnaca.

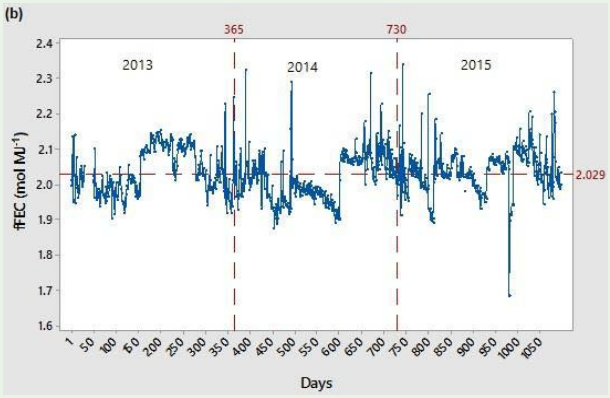

Figure 8b: Time series plots of the daily ratios of *fFEC* at Larnaca. Mean annual daily value of *fFEC* = 2.029 mol MJ^{-1}.

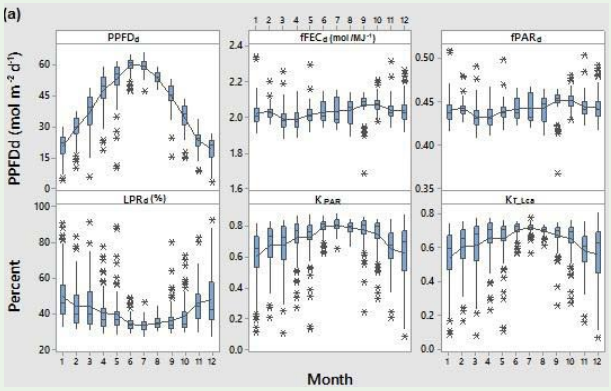

Figure 10a: Monthly daily PAR-related values using boxplots for $PPFD_d$, $fFEC_d$, $fPAR_d$, LPR_d, K_{PAR}, and K_T at Larnaca.

seen that the variation of the monthly values (continuous smooth curves) are quite regular, with maximum taking place in June and the minimum in December.

The average annual daily values (mean ± SE) over the study period of $PPFD_d$, $PARE_d$, G_d, $fPAR_d$, $fFEC_d$, LPR_d, K_T, and K_{PAR} were 40.26 ± 0.48 mol m^{-2} d^{-1}, 8.75 ± 0.11 MJ m^{-2}d^{-1}, 19.93 ± 0.24 MJ m^{-2}d^{-1}, 0.441 ± 0.0004, 2.029 ± 0.002 mol MJ^{-1}, 41.07 ± 0.35%, 0.643 ± 0.004, and 0.722 ± 0.004, respectively. The monthly means of the daily values of all PAR-related variables including their variability are shown in Figure 10a. The asterisks on the graphs indicate outliers of the given variables (observations that are beyond the upper or lower whisker). The monthly mean daily values of the variables $fPAR_d$ and $fFEC_d$ are relatively constant throughout the year. The lowest values of these variables are recorded in spring, with slightly higher values in autumn. The highest values of $PPFD_d$, $PARE_d$, G_d, and the clearness indices occur in summer and the lowest in winter. In contrast, LPR_d exhibited an opposite trend with the lowest values in the summer period. The highest variability is occurred in spring and winter months as indicated by the length of the box plots of the above variables. The monthly mean daily *PPFD* varied between 19.05 (the average in December) and 59.63 mol m^{-2} d^{-1} (the average in June). The monthly mean daily PAR*E* (Figure 10b) closely follows *PPFD*, ranging from 4.14 to 12.96 MJ m^{-2} d^{-1}. Global solar radiation (Figure 10b) exhibited a seasonal pattern similar to that of *PPFD* and PAR*E*, ranging from 9.44 to 29.53 MJ m^{-2} d^{-1}. *fFEC* ranged from 1.986 (in March and April) to 2.072 mol MJ^{-1} (in October), whereas the respective *f*PAR values ranged between 0.432 (in March and April) and 0.450 (in September and October), with an average daily value of 0.441. Almost similar results were obtained by Jacovides et al. [3,21] for Athalassa, an inland location in Cyprus and in Athens [13].

The monthly mean daily values of G_d, $PARE_d$, $fPAR_d$, $PPFD_d$ and $fFEC_d$ for each month, season and different sky conditions for the period of measurements are presented in Table 4. The results of the monthly and seasonal variations were discussed in previous paragraphs. Regarding the sky conditions, it is evident from the table that *f*PAR and *fFEC* are higher in overcast sky conditions (0.465 and 2.140 mol MJ^{-1}, respectively), while they obtain their lower values on clear days (0.439 and 2.020 mol MJ^{-1}, respectively). This result can be attributed to the fact that water vapour values during overcast conditions are affecting more the longer wavelengths through the absorption process, leaving the spectral PAR portion unaltered, thus, decreasing broadband solar radiation to a much greater extent than the spectral PAR; therefore, the ratios are increased with the increase of water vapour content [3, 12]. Figure 11 confirms the results of Table 4, i.e, for high K_T we expect lower *fFEC* and *f*PAR ratio. The relationship is in the form of $Y = aX^b$. The coefficients a and b have the following values: $a = 1.983$ and b=-0.048. The relationship of PAR*E* and global solar radiation for the three different sky conditions is shown in Figure 12. The average daily *PPFD* decreases from 47.5 mol m^{-2} d^{-1} on clear days to 11.7 mol m^{-2} d^{-1} on overcast days.

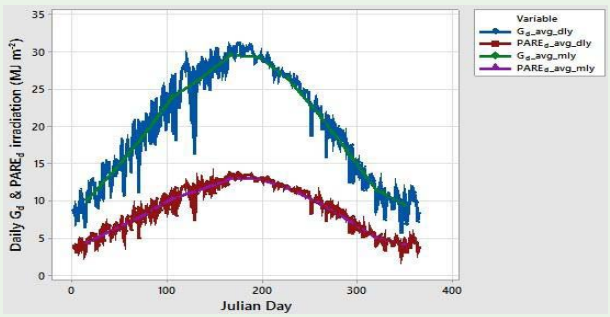

Figure 9: Annual evolution of daily and monthly *PAR* and global solar radiation for all skies (MJ m^{-2}), at Larnaca, Cyprus, for the period 2013-2015.

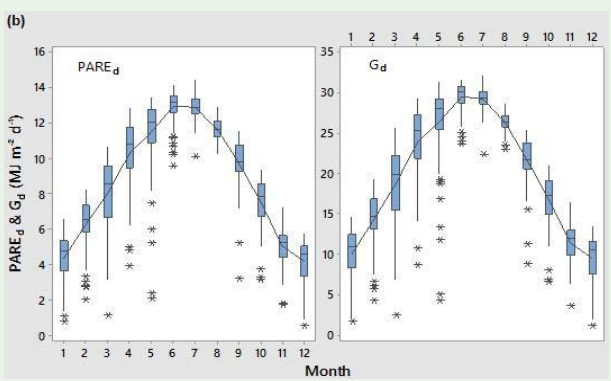

Figure 10b: Box plots of daily $PARE_d$ and Global solar radiation showing the monthly variability of the radiation variables at Larnaca.

Table 4: Monthly mean daily values of G_d, $PARE_d$, $fPAR_d$, $PPFD_d$ and $fFEC_d$ for each month, season and different sky conditions for the period of measurements at Larnaca.

Month	Gd	PAREd	fPARd	PPFDd	fFECd
	(MJ m^{-2} d^{-1})	(MJ m^{-2} d^{-1})		(mol m^{-2} d^{-1})	(mol MJ^{-1})
1	10.0	4.4	0.439	20.1	2.020
2	14.3	6.3	0.441	29.0	2.030
3	18.6	8.0	0.432	36.7	1.986
4	23.9	10.3	0.432	47.4	1.986
5	26.4	11.5	0.436	52.7	2.004
6	29.5	13.0	0.439	59.6	2.020
7	29.3	12.9	0.441	59.4	2.031
8	26.3	11.6	0.442	53.5	2.035
9	21.7	9.8	0.450	45.0	2.071
10	16.7	7.5	0.450	34.6	2.072
11	11.4	5.1	0.444	23.3	2.040
12	9.4	4.1	0.442	19.1	2.035
Year	19.9	8.8	0.441	40.3	2.027
Season					
1	10.9	4.8	0.441	22.1	2.028
2	22.9	9.9	0.433	45.6	1.992
3	28.4	12.5	0.441	57.5	2.029
4	16.6	7.4	0.448	34.3	2.061
Sky condtions					
Clear days	23.5	10.3	0.439	47.5	2.020
Partly cloudy	13.9	6.1	0.441	28.2	2.031
Overcast	5.6	2.5	0.465	11.7	2.140

Finally, the cumulative density functions (*CDF*) of the daily $PARE_d$,G_d irradiation and $PPFD_d$ are presented in Figure 13. The figure indicates that in 60% of the days $PARE_d$ is lower than 10.4 MJ m^{-2} and lower than 23.9 MJ m^{-2} for the global solar radiation. For the same probability level (60%) $PPFD_d$ is lower than 47.8 mol m^{-2} d^{-1}.

Statistical relationships with sunshine duration

The Angstrom-Prescott model [56] is the most widely used method for global radiation predictions. It is given as,

$$G_d = [a + b(n/N)]G_{0d} \quad (8)$$

G_d is the daily horizontal global solar irradiation on the ground surface, G_{0d} is the daily extraterrestrial solar irradiation on a horizontal surface at the top of the atmosphere, n/N is the relative sunshine duration, whereas a and b is regression constants. Using daily data for Larnaca Eq. (8) takes the form:

$$G_d = [0.261 + 0.528*(n/N)]G_{0d} \quad R^2 = 0.909 \quad (9)$$

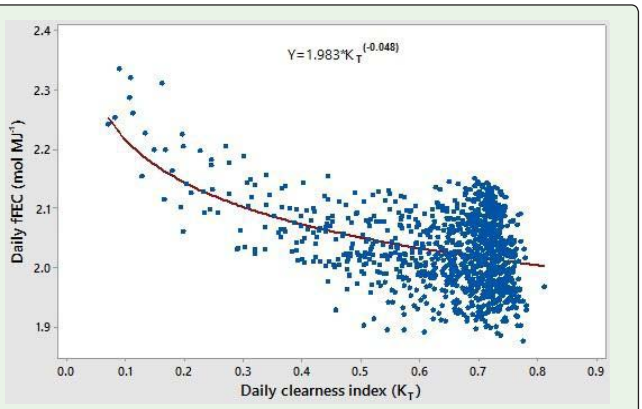

Figure 11: Relationship between daily $fFEC_d$ and daily clearness index at Larnaca.

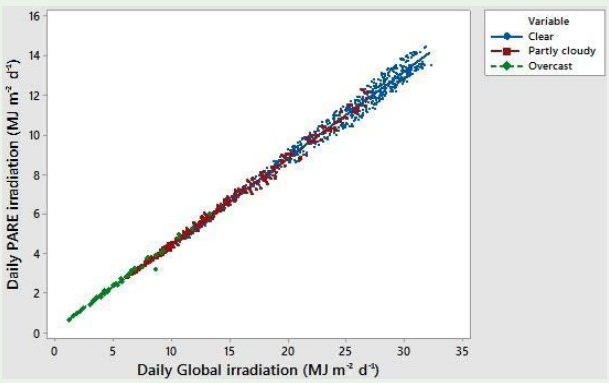

Figure 12: Relationships between $PARE_d$ and G_d irradiation for clear, partly cloudy and overcast sky conditions obtained from daily values at Larnaca.

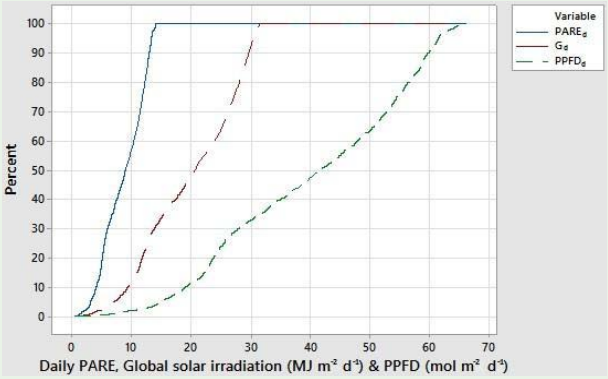

Figure 13: Cumulative Density Function (CDF) of the daily $PARE_d$, G_d irradiation and $PPFD_d$ at Larnaca.

As in the case of solar global irradiation, the PAR component is modelled by means of the Angstrom's type equation:

$$PPFD_d = [0.271 + 0.518*(n/N)]PPFD_{0d} \quad R^2 = 0.896 \qquad (10)$$

Where $PPFD_d$ is the daily *PPFD* value in photobiology units (mol m^{-2}), *n/N* is the sunshine fraction and $PPFD_{0d}$ is the daily extraterrestrial value at the top of the atmosphere. Almost similar regression constants were obtained by Jacovides et al. [30] for Athalassa, Cyprus.

Comparison of PAR measured at other locations in Cyprus

The daily values of global and photosynthetic active radiation were compared with the respective values of the other four stations. Figure 14 shows the monthly mean daily values of G_d, $PARE_d$, $PPFD_d$ and $fFEC_d$. The similarities between the stations are evident. Elevation plays a significant role on the values of the above variables. Generally, stations at higher elevation have lower values.

Linear relationships were fitted between the daily *PPFD* (mol m^{-2} d^{-1}) of Larnaca and the same variable of the above four stations:

$$PPFD_d\_Lca = 2.469 + 1.045*PPFD_d\_Par \quad R^2 = 0.945 \qquad (11)$$

$$PPFD_d\_Lca = 6.476 + 0.939*PPFD_d\_Cho \quad R^2 = 0.890 \qquad (12)$$

$$PPFD_d\_Lca = 7.749 + 0.981*PPFD_d\_Kal \quad R^2 = 0.832 \qquad (13)$$

$$PPFD_d\_Lca = 8.695 + 0.998*PPFD_d\_Far \quad R^2 = 0.830 \qquad (14)$$

The two coastal stations (Larnaca and Paralimni) show higher coefficient of determination (Eq. 11).

Relationship of PAR-related parameters with elevation: The relationship between the PAR-related parameters and elevation was examined for both hourly and daily data sets. The conventional way to analyse *fFEC* is to group them into different weather categories, e.g. clear, partly cloudy and cloudy. The criterion to select the given category is the clearness index, i.e., $k_t > 0.65$: clear, $0.35 < k_t < 0.65$: partly cloudy and $k_t < 0.35$: cloudy. Then, the mean values of the hourly PAR-related parameters for the whole period were calculated for each station and their values were plotted as a function of the elevation. Figure 15 shows the relationship of the means of *PPFD*,

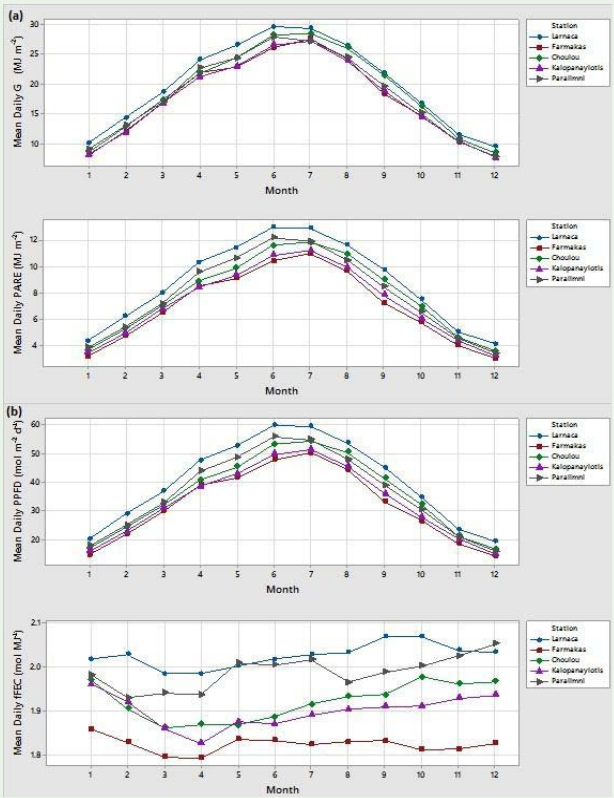

Figure 14: Monthly mean daily values of a) G_d and $PARE_d$, and b) $PPFD_d$ and $fFEC_d$ at different locations in Cyprus.

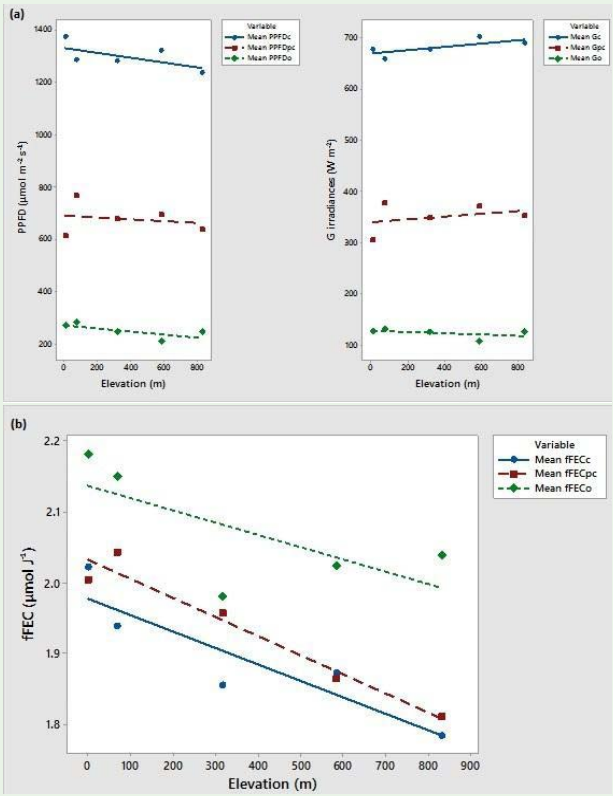

Figure 15: Relationships of the monthly mean hourly of a) *PPFD* and *G* and b) *fFEC* with elevation.

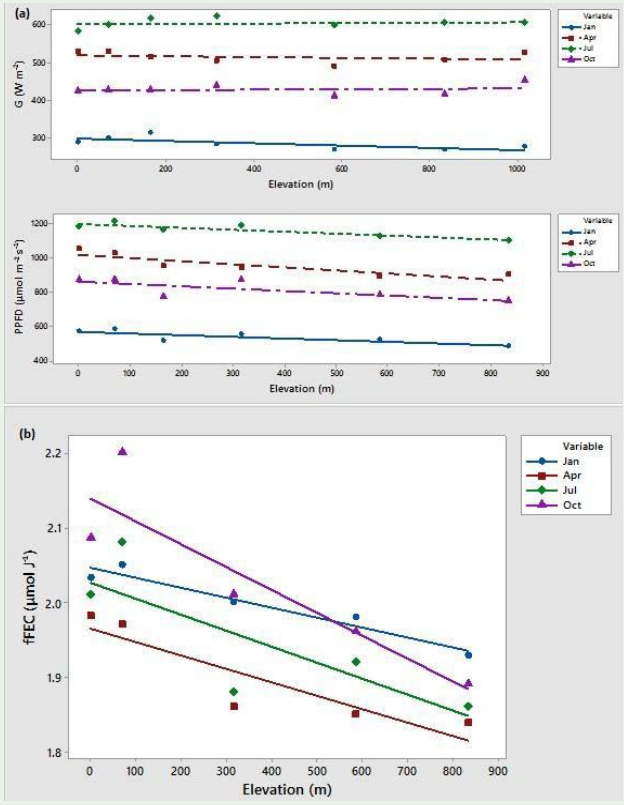

Figure 16: Relationships of the monthly mean values of a) *G* and *PPFD* and b) *fFEC* with elevation in different months.

G and *fFEC* with the elevation. *PPFD* is decreased with elevation for all the categories with almost a similar slope. A negative slope with elevation is also observed for *G* during cloudy conditions. However, *G* is increased with elevation in clear and partly cloudy conditions (Figure 15a). As a general trend, *fFEC* followed the order Clear<Partly cloudy<Cloudy (Figure 15b). In all cases *fFEC* was decreased with elevation but with a different rate. Similar results were obtained by Wang et al. [23] in Naeba Mountain in Japan.

Figure 16 shows the relationships of the monthly daily means of G_d, $PPFD_d$ and $fFEC_d$ with the elevation during different seasons of the year. A slight negative slope is observed for global irradiance in January, while in the other seasons the slope is zero or slightly positive. On the other hand, *PPFD* is decreased with elevation with almost similar slope in all the months (Figure 16a). As a result, $fFEC_d$ is decreased with elevation, but with a different rate in winter months. During the rest of the months the lines are almost parallel (Figure 16b).

Modelling photosynthetic active radiation

Previous research results show that parameterization models that use atmospheric parameters measured at meteorological stations can generate accurate PAR estimates [3,12,14,57]. Six models obtained from the literature will be developed and tested under Cyprus conditions. The first three are linear or multilinear models, and the rest three have a power form.

Aguiar et al. [14] have proposed three multilinear regression models to estimate PAR based on parameters routinely measured in meteorological stations. These variables were chosen due to their presumed influence on PAR as it was demonstrated by [11-13]. The chosen variables are the global solar irradiance (model 1), global solar irradiance and clearness index (model 2), and global irradiance, clearness index and water vapour pressure (model 3). The models differ in their complexity by adding additional variables. The clearness index can represent the combined attenuation effects of aerosols, gases and cloud cover on solar radiation transfer through the atmosphere. The regression equations of the three models have the following form:

$$PARE = a*G \quad (15)$$

$$PARE = a*G + b*k_t + c \quad (16)$$

$$PARE = a*G + b*k_t + c*e + d \quad (17)$$

Where, *G* is the hourly broadband solar irradiance (W m^{-2}), k_t is the clearness index (ratio of global to extraterrestrial solar irradiance) and *e* is the water vapour pressure (hPa). The regression parameters a, b, c and d were determined using multiple linear regressions for the period 2013-2014, while the year 2015 was used as a testing data set for the validation of the models. Daily and hourly extraterrestrial radiation was estimated by the earth-sun geometric relationships (Equation 3 and 4). The saturation water vapour pressure (e_s, hPa) was calculated from the Tetens equation [58] and the water vapour pressure was calculated using e_s and air relative humidity (*RH*, %).

Research findings show that PAR transmissivity k_{PAR}, k_t, and the solar zenith angle (through the relative optical air mass (*m*)) can be used to accurately estimate PAR values [57]. Non-dimensional parameters in the equation eliminate local feature effects. The parameterization model for estimating PAR (model 4) takes the following form:

$$k_{PAR} = a*k_t^b*m^c \quad (18)$$

The relative optical air mass (*m*) is defined as the direct optical path length through the Earth's atmosphere. The formula obtained from Kasten and Young [59] is used to estimate *m* by using the solar zenith angle (θ_z):

$$m = 1/(\cos\theta_z + 0.050572(96.0795 - \theta_z)^{-1.6364} \quad (19)$$

Therefore, model 4 takes the following form:

$$PARE = (a*k_t^b*m^c)*PARE_0 \quad (20)$$

Where $PARE_0$ is the extraterrestrial PAR irradiance.

The next model (model 5) takes into account the effect of the comprehensive attenuation factors under clear skies (ρ_c) and the effect of clouds through the global clearness index and has the following form:

$$k_{PAR} = a*\rho_c^b*k_t^c \quad (21)$$

The index ρ_c is calculated using the following equation:

$$\rho_c = PARE_c / PARE_0 \quad (22)$$

Where $PARE_c$ represents the observed PAR under clear weather conditions. $PARE_c$ can be estimated using any radiative transfer model or through empirical models. In this study $PARE_c$ is estimated from the relative optical air mass value as shown in figure 17. A

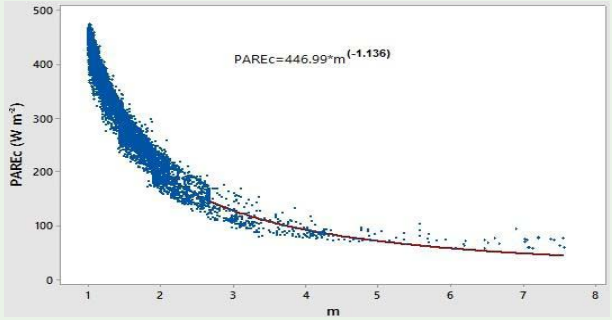

Figure 17: The dependence of PARE values on *m* for clear weather conditions ($k_t > 0.65$) at Larnaca.

small degree of dispersion is evident between PAR values under clear weather and m conditions. The equation which describes the relationship between $PARE_c$ and the relative optical air mass (m) under clear weather conditions, i.e., $k_t > 0.65$ has the following form:

$$PPFD_c = 2056.8 * m^{-1.136} \quad (\mu mol\ m^{-2}\ s^{-1}) \qquad (23a)$$

or

$$PARE_c = 446.99 * m^{-1.136} \quad (W\ m^{-2}) \qquad (23b)$$

Essentially, the final form of model (5) is shown below:

$$PARE = (a * \rho_c^b * k_t^c) * PARE_0 \qquad (24)$$

The 6th model was proposed by Wang et al. [39] and expresses the relationship between hourly PAR and the cosine of solar zenith angle for a very narrow range of k_t interval, and can be described as follows:

$$PARE = PARE_x * (\cos(\theta_z))^a \qquad (25)$$

Figure 18 shows the dependences of hourly PAR on k_t and the cosine of solar zenith angle. PAR is increased almost exponentially with cos (SZA) for a given k_t interval, which is described with a power law equation (Eq. 25). Firstly, the maximum value $PARE_x$ is estimated by binning k_t in 0.02 increments. Then, the relationship between $PARE_x$ and k_t is established using a cubic polynomial function as shown in figure 19. The equation has the following form:

$$PPFD_x = 137.6 + 1163 * k_t + 3815 * k_t^2 - 2646 * k_t^3 \quad (\mu mol\ m^{-2}\ s^{-1}) \qquad (26a)$$

or

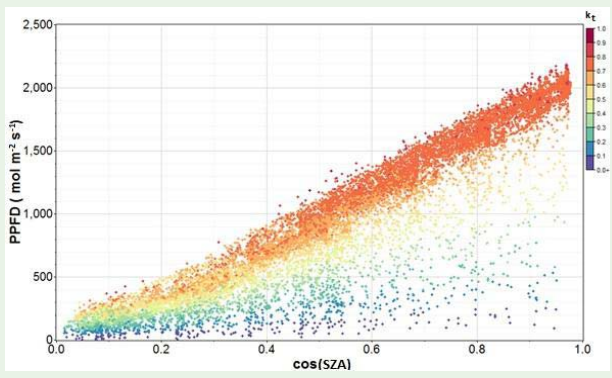

Figure 18: Hourly dependences of *PAR* on k_{PA} and the cosine of solar zenith angle at Larnaca.

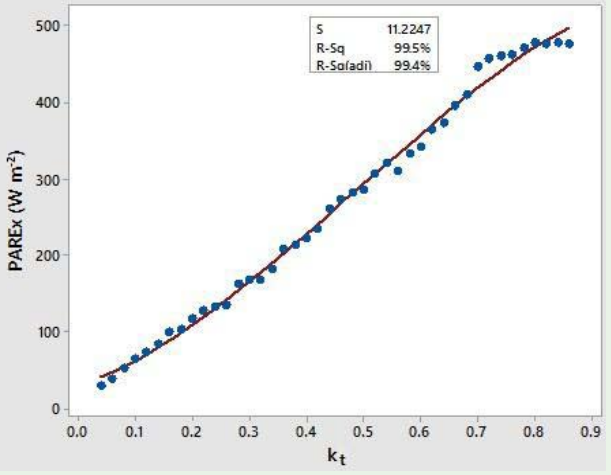

Figure 19: $PARE_x$ as a function of k_{PA} at Larnaca (it can be expressed as a cubic polynomial equation (Equations. 26a and 26b).

$$PARE_x = 30.12 + 254.4 * k_t + 834.9 * k_t^2 - 579 * k_t^3 \quad (W\ m^{-2}) \qquad (26b)$$

$$R^2 = 0.995$$

In the second step, b was obtained from analysing the relationship between hourly PAR and *cos(SZA)* using a non-linear statistical method.

Table 5 summarises the regression parameters (a, b, c, and d) of the six models which were used for the estimation of PAR. The linear and multilinear models show high coefficients of determination; the simple linear model showed the highest coefficient of determination amongst the first three models. Regarding the models which are based on the power law, model 4 showed the lowest *S* which indicates that the given equation predicts better the response variable. *S* is measured in the units of the response variable and represents the standard distance the data values fall from the regression line, or the standard deviation of the residuals. Furthermore, Table 5 shows the parameters of the equation which calculates the clear sky $PARE_c$ values and depends on the relative optical air mass (*m*) (Figure 17). $PARE_x$ is estimated using a cubic polynomial function of k_t with a very high coefficient of determination (R^2=0.995).

Validation of the models: To evaluate the developed models, the models were validated using the last year's PAR hourly data (2015) as an independent data set. Table 6 shows the results of the linear regression analysis between the estimated and measured PAR values for each model, including the slope *e*, intercept *f*, R^2, Mean Bias Error (MBE), Root Mean Square Error (RMSE) and Relative Error (RE). The statistical estimators *MBE*, *RMSE* and *RE* have the following form:

$$MBE = \frac{1}{n}\sum_{i=1}^{n}(E_i - M_i) \qquad (27)$$

$$RMSE = [\frac{1}{n}\sum_{i=1}^{n}(E_i - M_i)^2]^{0.5} \qquad (28)$$

$$RE(\%) = \sum_{i=1}^{n}(|M_i - E_i|/M_i) * 100/n \qquad (29)$$

Table 5: Regression parameters of the proposed six models, based on hourly data during the period 2013-2015 at Larnaca.

Models	Equation	Parameters	Type	a	b	c	d	R^2/S
Model_1	15	G	Linear	0.440				R^2 = 0.998
Model_2	16	G, k_t	Multilinear	0.451	-17.760	5.434		R^2 = 0.993
Model_3	17	G, k_t, e	Multilinear	0.449	-16.66	0.257	1.134	R^2 = 0.993
Model_4	18	k_t, m	Power	0.934	0.962	-0.021		S = 0.0245
PAREc	23b	m	Power	446.99	-1.136			S=19.114
Model_5	24	ρ_c, k_t	Power	0.985	0.178	0.942		S=10.435
PAREx	26b	k_t	Cubic	30.12	254.4	834.9	-579.0	R^2=0.995
Model_6	25	k_t, cos (SZA)	Power	0.996				S=16.240

Table 6: Validations of estimated hourly *PAR* under all sky conditions using the validation data set of the year 2015 at Larnaca, where *e* and *f* is the slope and the intercept of linear regression of estimated vs measured *PAR* values. *MBE* and *RMSE* are expressed in W m^{-2}.

Models	e	f	R^2	MBE	RMSE	RE (%)
Model_1	0.985	2.641	0.996	-0.046	7.904	3.78
Model_2	0.988	1.999	0.996	-0.576	7.823	3.29
Model_3	0.988	1.829	0.996	-0.821	7.899	3.35
Model_4	0.994	-0.468	0.995	-1.789	8.707	4.49
Model_5	0.995	-0.073	0.996	-1.224	8.361	4.14
Model_6	1.008	-3.048	0.986	-1.368	15.071	8.37

Where *n* is the number of data pairs, E_i is the ith estimated PAR irradiance with the given model, and M_i is the ith measured PAR irradiance value.

All the models underestimate slightly PAR hourly values as it is indicated by the negative values of *MBE*. All the models showed high coefficients of determination (R^2) (close to 1), which indicates that the proposed models are suitable for predicting hourly PAR values. The linear and multilinear models (models 1 to 3) have the same coefficient of determination. The relative error values for the first five models range between 3.3% and 4.5%, while the sixth model showed higher relative error (8.4%). In all cases the slopes of the linear regressions are close to 1. Therefore, the performances of the linear and multilinear models are superior with respect to their relative errors. The power law models (4 to 6) are mainly based on the estimation of k_t and k_{PAR} indices.

Conclusion

PAR is a key parameter that controls many physical and ecological processes. PAR is an essential parameter used in studies on radiation balance and agrometeorological modelling. Therefore, the study of PAR variability and the development of PAR estimation method are critical in climate research and ecological modelling. It is expressed either in terms of photosynthetic photon flux density (*PPFD*, μmol m^{-2} s^{-1}), since photosynthesis is a quantum process, or in terms of photosynthetic radiation flux density (PAR irradiance, W m^{-2}), which is more suitable for energy balance studies. It can be also expressed as a fractional energy of PAR to global solar radiation (*f*PAR), or as a fraction of photon flux/energy conversion of PAR (*fFEC*, μmol J^{-1} or mol MJ^{-1}). In this study, three years of hourly PAR and global irradiance measured at Larnaca (coastal location) are used to examine daily/monthly PAR variations at this station. Furthermore, the study compares the PAR values and the above ratios with other stations operated in different climate conditions.

The first objective of this study is the quality control of PAR values at the measuring stations. The quality control process was based on physically possible limits, such as the measured PAR values must be lower than the PAR flux at the top of the atmosphere and the ratio PAR/*G* (*fFEC*) must fall between 1.3 and 2.8 mol MJ^{-1}[52]. All data that do not meet the conditions specified by the suggested tests are not used in the study.

The second objective of this study is the analysis of the statistical characteristics of both hourly and daily values of PAR related parameters including the statistical relationships between PAR and other radiation components. The annual mean daily PAR value for Larnaca is about 40 mol m^{-2} d^{-1}, while in the rest observation sites it ranged between 31.7 to 36.9mol m^{-2} d^{-1}. The highest values are recorded in the coastal stations (Larnaca and Paralimni). Monthly average daily PAR increased from 19.1 mol m^{-2} d^{-1} (in December) to 59.6 mol m^{-2} d^{-1} (in June). The annual average value of *fFEC* at the five observation sites ranges from 1.82 to 2.03 molM J^{-1}, in accordance to what is observed in most parts of the world. The highest appeared in the coastal sites of Larnaca and Paralimni due to the presence of high water vapour atmospheric concentrations. The monthly daily average at Larnaca of *fFEC* remained almost constant throughout the year. It was also discovered that *fFEC* generally decreased with sky conditions changing from overcast skies to clear skies (Table 4 and Figure 11), which may due to the strong absorption and scattering effects of clouds on longer wavelengths.

Elevation plays a significant role on the values of the above variables. As a general trend, *fFEC* followed the order Clear<Partly cloudy<Cloudy (Figure 15b). In all cases *fFEC* was decreased with elevation but with a different rate. A slight negative slope is observed for global radiation in January, while in the other seasons the slope is zero or slightly positive. On the other hand, *PPFD* is decreased with elevation with almost similar slope in all the months (Figure 16a).

The third objective was to evaluate the performance of various models in estimating PAR irradiances under all-sky conditions. For this purpose, the first two years of the data were used as a training data set to calibrate well known models and the last year's data were used to evaluate the performance of the selected models to calculate PAR values. The parameterizing process for the hourly data set was implemented for the coastal station of Larnaca. For this purposes, one linear, two multilinear and three power low models were investigated. The linear model was based on the close relationship between PAR and global irradiance, while the multilinear models are based also on clearness index and water vapour pressure. On the other hand the power law models are mainly based on the clearness index, optical air mass and the cosine of the solar zenith angle, i.e., on factors which affect the transmissivity of the solar radiation through the atmosphere.

The performance of the models was based on the coefficient of determination (R^2), the Mean Bias Error (MBE), the Root Mean Square Error (RMSE) and the Relative Error (RE) between the estimated and measured hourly values. All the models showed high coefficients of determination (R^2) (close to 1), which indicates that the proposed models are suitable for predicting hourly PAR values. The linear and multilinear models (models 1 to 3) have the same coefficient of determination (0.996). The relative error values for the first five models ranged between 3.3% and 4.5%, while the sixth model showed higher relative error (8.4%). In all cases the slopes of the linear regressions are close to 1. Therefore, the performances of the linear and multilinear models are superior with respect to their relative errors.

The analysis of this article improves our understanding of PAR variability and its relationship with *G* under various sky conditions in Cyprus. The proposed models may play fundamental role in many fields such as terrestrial ecosystem processes, atmospheric environment and agricultural production. Moreover, the models should be tested with data from the rest observation sites which have different climate conditions. Since most meteorological stations are equipped with global solar radiation sensors, then the developed models can be used to estimate accurately PAR irradiances at various locations in Cyprus. Therefore, the productivity of the different regions of the island could be effectively assessed.

Nomenclature:

CDF	Cumulative density function
cf	Conversion factor (4.57 μmol J^{-1})
e	Screen level water vapour pressure (hPa)
e_s	Saturated screen level water vapour pressure (hPa)
E_i	Estimated irradiance [W m^{-2}]
fFEC	Fraction of photon flux to energy conversion of PAR [μmol J^{-1}] (PAR/G)
$fFEC_d$	Daily fraction of photon flux to energy conversion of PAR [$molMJ^{-1}$]
*f*PAR	Fractional energy of PAR to global solar radiation
$fPAR_d$	Daily fractional energy of PAR to global solar radiation
G	Global solar irradiance [W m^{-2}]
G_d	Daily global solar irradiation [MJ m^{-2}]
G_0	Extraterrestrial irradiance [W m^{-2}]
G_{0d}	Daily extraterrestrial irradiation (ETR) [MJ m^{-2}]
G_{sc}	Solar constant [1367 W m^{-2}]
k_t	Hourly clearness index (G/G_0)
K_T	Daily clearness index (G_d/G_{0d})
k_{PAR}	Hourly PAR clearness index (PAR/PAR_0)
K_{PAR}	Daily PAR clearness index (PAR_d/PAR_{0d})
L	Eccentricity
LPR	Lost PAR radiation (%)
m	Optical air mass
M_i	Measured irradiance [W m^{-2}]
MBE	Mean Bias Error
n	Number of observations
N	Non missing observations
N^*	Missing observations
n/N	Daily relative sunshine duration
PAR	Photosynthetic active radiation
PAR_c	Clear sky photosynthetic active radiation
PAR_x	Maximum photosynthetic active radiation
PAR*E*	Photosynthetic active radiation flux density [W m^{-2}]
$PARE_c$	Clear sky photosynthetic active radiation flux density [W m^{-2}]
$PARE_x$	Maximum photosynthetic active radiation flux density [W m^{-2}]
$PARE_{sc}$	Photosynthetic active solar radiation constant (536.64 W m^{-2}]
$PARE_0$	Extraterrestrial photosynthetic active radiation flux density [W m^{-2}]
$PARE_d$	Daily photosynthetic active radiation [MJ m^{-2}]
$PARE_{0d}$	Daily extraterrestrial photosynthetic active radiation [MJ m^{-2}]
PPFD	Photosynthetic photon flux density [μmol m^{-2} s^{-1}] or [mol m^{-2} h^{-1}]
$PPFD_d$	Daily photosynthetic photon flux density [mol m^{-2} d^{-1}]
$PPFD_{sc}$	Photosynthetic active solar radiation constant [2443.3 μmol m^{-2} s^{-1}]
Q1	First Quartile
Q3	Third Quartile
RMSE	Root mean square error
RE	Relative error (%)

RH	Relative humidity (%)
R^2	Coefficient of determination
S	Standard deviation of residuals
SZA	Solar zenith angle (θ_z) [degrees]
$T\ (^0C)$	Air temperature at screen level (^{0}C),

Greek:

a_s	Solar elevation angle [degrees]
δ	Solar declination angle [degrees]
Δ	Brightness of the skylight
ε	Clearness of the sky
θ_z	Solar zenith angle [degrees]
ρ_c	Attenuation factor under clear skies
ϕ	Latitude angle [degrees]
ω_i	Hour angle [degrees]
ω_s	Sunset hour angle [degrees]

References

1. McCree KJ. Test of current definitions on photosynthetically active radiation. Agric Meteorol. 1972; 10: 443-453.
2. Alados I, Alados-Arboledas L. Direct and diffuse photosynthetically active radiation: measurements and modelling. Agric For Meteorol.1999; 93: 27-38.
3. Jacovides CP, Tymvios FS, Papaioannou G, Assimakopoulos DN, Theophilou CM. Ratio of PAR to global solar radiation measured in Cyprus. Agric For Meteorol. 2004; 121: 135-140.
4. Monteith JL. Climate variation and the growth of crops. Quart J R Met Soc. 1981; 107: 749-774.
5. Goudriaan J, van Laar HH. Modelling potential crop growth processes. textbook with exercises. Kluwer Academic Dordrecht. 1994; 238.
6. Monteith JL. Solar radiation and productivity in tropical ecosystems. J Appl Ecol. 1972; 9: 747-766.
7. Monteith JL, Moss CJ. Climate and the efficiency of crop production in Britain. Phil Trans R Soc London. 1977; 281: 277-294.
8. Jacovides CP, Tymvios FS, Assimakopoulos DN, Steven MD. Urban aerosol and clear skies spectra for global and diffuse photosynthetically active radiation. Agric For Meteorol. 1997; 87: 91-104.
9. Sinclair TR, Muchow RC. Radiation use efficiency. Adv Agron. 1999; 65: 215-265.
10. Udo SO, Aro TO. Global PAR related to global solar radiation for central Nigeria. Agr For Meteorol. 1999; 97: 21-31.
11. Tsubo M, Walker S. Relationships between photosynthetically active radiation and clearness index at Bloemfontein, South Africa. Theor Appl Climatol. 2005; 80: 17-25.
12. Alados I, Foyo-Moreno I, Alados-Arboledas L. Photosynthetically active radiation: measurements and modelling. Agric For Meteorol. 1996; 78: 121-131.
13. Jacovides CP, Tymvios F S. Assimakopoulos VD. Kaltsounides NA. The dependence of global and diffuse PAR radiation components on sky conditions at Athens, Greece. Agric For Meteorol. 2007; 143: 277-287.
14. Aguiar LJ, Fischer GR, Ladle RJ, Malhado A, Justino FB, Aguiar RG et al. Modeling the photosynthetically active radiation in South West Amazonia under all sky conditions. Theor Appl Climatol. 2012; 108: 631-640.
15. Shaokui Ge, Smith RG, Jacovides CP, Kramer MG, Carruthers RI. Dynamics of photosynthetic photon flux density (PPFD) and estimates in coastal northern California. Theor Appl Climatol. 2011; 105: 107-118.
16. Mc Cree KJ. The action spectrum, absorptance and quantum yield of photosynthesis in crop plants. Agr Forest Meteorol. 1972; 9: 191-216.
17. Dye DG. Spectral composition and quanta-to-energy ratio of diffuse photosynthetically active radiation under diverse cloud conditions. J Geophys Res. 2004; 109: 1-12.
18. Alados I, Olmo FJ, Foyo-Moreno I, Alados-Arboledas L. Estimation of photosynthetically active radiation under cloudy conditions. Agric For Meteorol. 2000; 102: 39-50.
19. Spitters CJT, Toussaint H, Goudriaan J. Separating the diffuse and direct component of global radiation and its implications for modeling canopy photosynthesis. Agr Forest Meteorol. 1986; 38: 217-229.
20. Papaioannou G, Papanikolaou N, Retalis D. Relationships of photosynthetically active radiation and shortwave irradiance. Theor Appl Climatol.1993; 48: 23-27.
21. Jacovides CP, Tymvios FS, Assimakopoulos DN, Theophilou KM. Global photosynthetically active radiation and its relationship with global solar radiation in the Easten Mediterranean basin. Theor Appl Climatol. 2003; 74: 227-233.
22. McCree KJ. A solarimeter for measuring photosynthetically active radiation. Agric Meteorol.1966; 3: 353-366.
23. Wang Q, Kakubari Y, Kubota M, Tenhunen J. Variation on PAR to global solar radiation ratio along altitude gradient in Naeba Mountain. Theor Appl Climatol. 2007; 87: 239-253.
24. Gueymard C. An atmospheric transmittance model for the calculation of the clear sky beam, diffuse and globalphotosynthetically active radiation. Agric For Meteorol. 1989; 45: 215-229.
25. Gueymard C. A Two-band model for the calculation of clear sky solar irradiance, illuminance, and photosynthetically active radiation at the earth's surface. Solar Energy.1989; 43: 253-265.
26. Gueymard C. Simple Model of the Atmospheric Radiative Transfer of Sunshine, version 2 (SMARTS2): Algorithms description and performance assessment. Report FSEC-PF-270-95, Florida Solar Energy Center.1995.
27. Alados-Arboledas L, Olmo FJ, Alados I, Pérez M. Parametric models to estimate photosynthetically active radiation in Spain. Agric For Meteorol. 2000; 101: 187-201.
28. Alados I, Foyo-Moreno I, Olmo FJ, Alados-Arboledas L. Improved estimation of diffuse photosynthetically active radiation using two spectral models. Agric For Meteorol. 2002; 111: 1-12.
29. Tyraski A, Papaioannou G, Retalis D, Gueymard C. Estimation of photosynthetically active radiation in Athens. In Proceedings of the 7th Panhellenic (International) Conference of Meteorology, Climatology and Atmospheric Physics. 2004; 1013-1020.
30. Jacovides CP, Tymvios FS, Boland J, Tsitouri M. Artificial Neural Network models for estimating daily solar global UV, PAR and broadband radiant fluxes in an eastern Mediterranean site. Atmospheric Research. 2015; 152: 138-145.
31. Pinker RT, Laszlo I. Global distribution of photosynthetically active radiation as observed from satellites. J Clim. 1992; 5: 56-65.
32. Frouin R, Pinker RT. Estimating photosynthetically active radiation (PAR) at the earth's surface from satellite observations. Remote Sens. Environ.1995; 51: 98-107.
33. Myneni RB, Hoffman S, Knyazikhin Y, Privette JL, Glassy J, Tian Y, et al. Global products of vegetation leaf area and fraction absorbed PAR from year

one of MODIS data. Remote Sens Environ. 2002; 83: 214-231.

34. Fensholt R, Sandholt I, Rasmussen MS. Evaluation of MODIS LAI, fAPAR and the relation between fAPAR and NDVI in a semi-arid environment using in situ measurements. Remote Sens Environ. 2004; 91: 490-507.

35. Bacour C, Baret F, Beal D, Weiss M, Pavageau K. Neural network estimation of LAI, fAPAR, fCover and LAIxC_{ab} from top of canopy MERIS reflectance data: Principles and validation. Remote Sens Environ. 2006; 105: 313-325.

36. Kathilankal JC, O'Halloran TL, Schmidt A, Hanson CV, Law BE. Development of semi-parametric PAR (Photosynthetically Active Radiation) partitioning model for the United States, version 1.0.Geoscientific Model Development. 2014; 7: 2477-2484.

37. Alados I, Alados-Arboledas L. Validation of an empirical model for photosynthetically active radiation. Int J Climatol. 1999; 19: 1145-1152.

38. Wang L, Wei G, Yingying M, Hu B, Zhang M. Photosynthetically active radiation and its relationship with global solar radiation in Central China. Int J Biometeorol. 2014; 58: 1265-1277.

39. Wang L, Wei G, Feng L, Lin A, Hu B, Zhou M. Estimation of hourly and daily photosynthetically active radiation in Inner Mongolia, China, from 1990 to 2012. Int J of Climatology. 2015; 35: 3120-3131.

40. Hu B, Yu Y, Liu Z, Wang Y. Analysis photosynthetically active radiation and applied parameterization model for estimating of PAR in the North China Plain. J Atmos Chem. 2016; 73: 345-362

41. Jacovides C, Kaltsunides N, Hachioannou L, Stefanou L. An assessment of the solar radiation climate of the Cyprus environment. Renewable Energy. 1993; 3: 913-918.

42. Petrakis M, Kambezidis C, Lycoudis S, Adamopoulos A, Kassomenos P, Michaelides I, et al. Generation of a 'typical meteorological year' for Nicosia, Cyprus. Renewable Energy. 1998; 13: 381-388.

43. Kalogirou S, Pashiardis S, Pashiardi A. Statistical analysis and inter-comparison of the global solar radiation at two sites in Cyprus. Renewable Energy. 2017; 101: 1102-1123.

44. Pashiardis S, Kalogirou SA, Pelengaris A. Statistical analysis and characterization of solar energy utilization and inter-comparison of solar radiation at two sites in Cyprus. Renewable Energy.2017; 190, 1138-1158.

45. Jacovides CP, Boland J, Assimakopoulos DN, Kaltsounides NA. Comparing diffuse radiation models with one predictor for partitioning incident PAR radiation into its diffuse component in the eastern Mediterranean basin. Renewable Energy. 2010; 35: 1820-1827.

46. Tymvios F, Jacovides C, Michaelides S, Tymvios V, Skouteli C. Direct and diffuse photosynthetically active radiation (PAR) for Nicosia-Cyprus.In Proceedings of the 7th Panhellenic (International) Conference of Meteorology, Climatology and Atmospheric Physics. 2004; 963-971.

47. World Meteorological Organization. WMO, 1987. Guidelines on the quality control of data from the World Radiometric Network. WCDP-3, WMO/TD-No.258, p 30, WMO, Geneva, Switzerland.

48. Muneer T. Solar Radiation and Daylight models. 2004.

49. Long C.N. and Dutton E.G. 2002. Global Network recommended QC tests, V2.0, BSRN Technical Report (http://ezksun3.ethz.ch/bsrn/admin/dokus/qualitycheck.pdf).

50. Long CN, Shi Y. An automated quality assessment and control algorithm for surface radiation measurements. The Open Atmospheric Science Journal 2008; 2: 23-37.

51. Pashiardis S and Kalogirou S. Quality control of solar shortwave and terrestrial longwave radiation for surface radiation measurements at two sites in Cyprus. Renewable Energy. 2016; 96: 1015-1033.

52. Hu B, Wang YS, Liu GR. The spatio-temporal characteristics of photosynthetically active radiation in China. J Geo phys Res. 2007; 112.

53. Iqbal M. An introduction to Solar radiation. Academic Press. 1983.

54. Gueymard C. The sun's total and spectral irradiance for solar energy applications and solar radiation models. Solar Energy. 2004; 76: 423-453.

55. Monteith JL, Unsworth MH. Principles of environmental physics, 2nd ed. Edward Arnold, London, United Kingtom.1990.

56. Black JN, Bonython CW, Prescott JA. Solar radiation and the duration of sunshine. Quart J Roy Met Soc. 1954; 80: 231-235.

57. Hu B, Wang YS. Comparison of multi-empirical estimation models of photosynthetically active radiation in Northeast China. Theor Appl Climatol. 2014; 116: 119-129.

58. Stull RB. Meteorology for Scientists and Engineers. Brooks/Cole Thomson Learning. 2000.

59. Kasten F, Young AT. Revised optical air mass tables and approximation formula. Appl Opt. 1989; 28: 4735-4738.